

## Characteristics of a turbulent boundary layer with an external turbulent uniform shear flow

By Q. A. AHMAD, R. E. LUXTON†  
AND R. A. ANTONIA‡

Department of Mechanical Engineering,  
University of Sydney, New South Wales 2006, Australia

(Received 22 October 1975 and in revised form 18 May 1976)

Measurements are presented of both mean and fluctuating velocity components in a turbulent boundary layer subjected to a nearly homogeneous external turbulent shear flow. The Reynolds shear stress in the external shear flow is small compared with the wall shear stress. Its transverse mean velocity gradient  $\lambda$  ( $\approx 6 \text{ s}^{-1}$ ) is also small compared with typical gradients based on outer variables (say  $U_w/\delta$ , where  $U_w$  is the value of the linear velocity profile extrapolated to the wall and  $\delta$  is the boundary-layer thickness), but is of the same order as  $U_\tau/\delta$  ( $U_\tau$  is the friction velocity). The influence of both positive and negative transverse velocity gradients on the turbulent wall layer is investigated over a streamwise region where the normal Reynolds stresses in the external flow are approximately equal and constant in the streamwise direction. In this region, the integral length scale of the external flow is of the same order of magnitude as that of the wall layer. Measurements in the boundary layer are also given for an un-sheared external turbulent flow ( $\lambda = 0$ ) with a turbulence level  $T_u$  of 1.5%, approximately the same as that for  $\lambda = \pm 6 \text{ s}^{-1}$ . ( $T_u$  is defined as the ratio of the r.m.s. longitudinal velocity fluctuation to  $U_w$ .) The measurements are in good agreement with those available in the literature for a similar free-stream turbulence level and show that the external turbulence level and length scale exert a large influence on the turbulence structure in the boundary layer. The additional effect of the external shear on the mean velocity and turbulent energy budget distributions in the inner region of the boundary layer is found to be small. In the outer region, the 'wake' component of the mean velocity defect is lowered by the presence of free-stream turbulence and one extra effect due to the external shear is an increase in the Reynolds shear stress when  $\lambda$  is positive and a decrease when  $\lambda$  is negative. Another interesting effect due to the shear is the appearance near the edge of the layer of a small but distinct region where the local mean velocity is constant and the Reynolds shear stress is negligible.

---

† Present address: Department of Mechanical Engineering, University of Adelaide, South Australia 5001.

‡ Present address: Department of Mechanical Engineering, University of Newcastle, New South Wales 2308, Australia.

## 1. Introduction

The study of the interaction of an external turbulent shear flow with the flow near the surface of bodies and structures on the earth's surface is of great importance. The present investigation considers the effect of a turbulent shear flow with a constant velocity gradient on the behaviour and structure of a turbulent boundary layer on a smooth surface. Apart from its importance to the atmosphere this investigation is also relevant to complex laboratory flows, such as the interaction between turbulent shear flows, or to turbomachinery flow, where the boundary layer on the rotor blade is in constant interaction with the external turbulent shear flow. Of more basic interest, however, is the possibility that the response of the boundary layer to this new outer boundary condition may shed further light on the turbulence structure of the layer. In the present investigation the length scale of the external shear flow is of the same order as that of the boundary layer and, as is typical in physical systems and as was pointed out by Bradshaw (1974), there is a chance that flows with comparable length scales will interact strongly.

The uniform shear flow used for the present experiments was that used by Mulhearn & Luxton (1975) and described in detail by Mulhearn (1971). The stream rate†  $\lambda = \partial U/\partial y = 6 \text{ s}^{-1}$  is a little smaller than that used by Rose (1966, 1970), Champagne, Harris & Corrsin (1970), Hwang (1971) and Richards (1971) and significantly smaller than that used by Masuda *et al.* (1972), but the turbulence characteristics are well documented and suggest that there is a good approximation to a quasi-homogeneous shear over a useful streamwise distance. In all uniform shear flows in which length scales have been measured it is found that all length scales, with the possible exception of that associated with the shear stress, grow monotonically downstream. The characteristics of the uniform shear flow are briefly reviewed in §2. In this paper, the term 'boundary layer' is retained in an attempt to distinguish between the external uniform shear flow and the shear flow in the vicinity of the wall. A definition of the boundary-layer thickness is given in §3. The mean velocity and turbulence data are presented in §§5 and 6 respectively. The turbulence length scales are also discussed in §6.

## 2. Characteristics of external uniform shear flow

As there is no asymptotic state in which a truly homogeneous turbulent flow exists in the presence of a uniform shear, and since the large-scale structure of a turbulent boundary layer is known to have a long 'memory', it is appropriate to discuss briefly the streamwise development and characteristic features of the present uniform shear flow and to compare these with those already reported in the literature. The measurements in the present uniform shear flow agree well with those of Mulhearn (1971), and show almost the same streamwise development.

Previous investigations of a uniform shear flow all show that both integral

† It would be more useful to quote strain rates in the form  $\lambda M^2/\nu$ , where  $M$  is representative of the initial length scale of the flow, but unfortunately  $M$  is either not recoverable from the published data or is not unique.

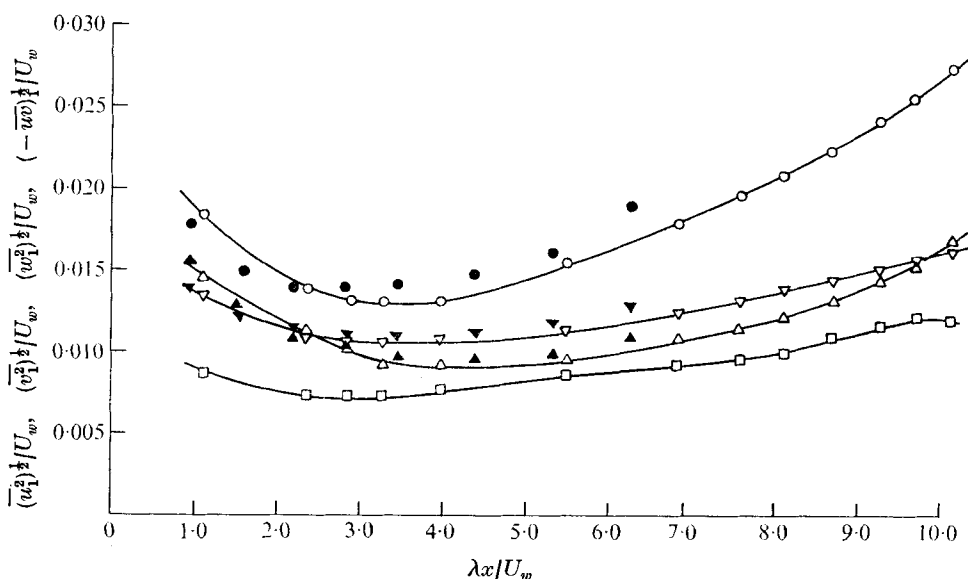


FIGURE 1. Streamwise development of Reynolds stresses. ●,  $(\overline{u_1^2})^{1/2}/U_w$ ; ▲,  $(\overline{v_1^2})^{1/2}/U_w$ ; ▼,  $(\overline{w_1^2})^{1/2}/U_w$ . Reynolds-stress data (Mulhearn & Luxton 1970): ○,  $(\overline{u_1^2})^{1/2}/U_w$ ; △,  $(\overline{v_1^2})^{1/2}/U_w$ ; ▽,  $(\overline{w_1^2})^{1/2}/U_w$ ; □,  $(-\overline{uw})_1/U_w$ .

length scales and Taylor microscales grow continuously in the  $x$  direction. Although in the present and in Mulhearn & Luxton's (1970) investigations  $\lambda$  ( $\sim 6 \text{ s}^{-1}$ ) is smaller than that used in other investigations, the maximum total mean strain (defined as  $x\lambda/U_c$ , where  $U_c$  is the mean velocity at  $y/h = 0.5$ ,  $h$  being the width of the working section) which can be achieved is in excess of 7 instead of the previous maximum value of 3.3 (Champagne *et al.* 1970). In all these investigations it is found that, after an initial period dominated by the decay of the turbulence generated by the shear-flow generating device (including the honeycomb), the Reynolds stresses appear to reach a constant value in the region of  $x\lambda/U_c = 3$ . However the Reynolds stresses subsequently increase at an increasing rate at larger total strains. Mulhearn & Luxton (1970) interpret this increase as a result of the reduced dissipation rate associated with the increasing length scales, with no compensating reduction in the production rate. Figure 1 shows the distribution of  $(\overline{u_1^2})^{1/2}/U_w$ ,  $(\overline{v_1^2})^{1/2}/U_w$  and  $(\overline{w_1^2})^{1/2}/U_w$  for the present investigation and  $(\overline{u_1^2})^{1/2}/U_w$ ,  $(\overline{v_1^2})^{1/2}/U_w$ ,  $(\overline{w_1^2})^{1/2}/U_w$  and  $(-\overline{uw})_1/U_w$  from Mulhearn & Luxton (1970), where  $u_1^2$ ,  $v_1^2$  and  $w_1^2$  are the turbulence intensities in the  $x$ ,  $y$  and  $z$  directions respectively,  $(-\overline{uw})_1$  is the kinematic shear stress along the centre-line of the tunnel and  $U_w$  is the 'slip' velocity in the  $x$  direction at the wall. These data indicate that  $\overline{u_1^2}$ ,  $\overline{w_1^2}$  and  $(-\overline{uw})_1$  begin to increase at  $x\lambda/U_c \approx 3.6$  but  $\overline{v_1^2}$ , which is initially larger than  $\overline{w_1^2}$ , does not increase until  $x\lambda/U_c$  reaches 6.4. This appears reasonable as all the turbulent energy goes first into the streamwise component, from which it is then distributed to other components. It seems that transfer to the  $\overline{w_1^2}$  component is preferred to transfer to the  $\overline{v_1^2}$  component as the latter is inhibited by the mean shear. It is worth noting that the streamwise rate of

increase of  $\overline{u_1^2}$  for  $x\lambda/U_c > 4$  is significantly larger than that for  $\overline{w_1^2}$  and  $\overline{v_1^2}$ , possibly indicating that pressure fluctuations at the Reynolds number of these experiments are relatively ineffective in distributing energy. The levels attained by the Reynolds stresses in the quasi-equilibrium region of the flow are not only determined by initial conditions (e.g. initial length scales as suggested by Rose 1970) but also by the total strain to which the flow is subjected. Mulhearn & Luxton (1975) observed that, because of the preferential amplification of some eddy structures by the external shear, information about the initial conditions other than about the length scale is destroyed after a total strain of about 1.5.

Support for results of Mulhearn & Luxton (1970) have been provided by Richards (1971), who investigated the characteristics of shear flows with both linear ( $\lambda = 15.6 \text{ s}^{-1}$ ) and quadratic ( $d\lambda/dy = \pm 2 \text{ m}^{-1} \text{ s}^{-1}$ ) velocity profiles with a maximum total strain of 5.6. Richards found that  $\overline{v_1^2}$  does not begin to rise until  $x\lambda/U_c$  exceeds 5.6 whilst the other stresses begin to increase at  $x\lambda/U_c \simeq 3.1$ . However, in the flows of Mulhearn & Luxton and also Richards, the lateral extent of the uniformly sheared region is not sufficiently large at downstream locations to be absolutely sure that the rapid growth of the turbulence energy is not stimulated by the boundary layers on the tunnel walls.

Lateral homogeneity of the Reynolds stresses and length scales has been checked by Mulhearn (1971) and found to be satisfactory for  $x/h < 16$ . Beyond this station the lateral length scales in the shear flow become comparable with the lateral extent of the uniformly sheared region and this suggests that the boundary-layer inhomogeneities influence the shear flow. For the present work these complications have been avoided by confining the investigation of the boundary layer to the range  $3.75 < x/h < 10$ , in which both streamwise and lateral variations of the stresses are checked experimentally and found to be negligible. The turbulent characteristics of the negatively sheared flow

$$(\lambda = -6 \text{ s}^{-1})$$

have been explored in detail only in the range  $4 < x/h < 8$  for  $U_c = 5.8 \text{ ms}^{-1}$ .

### 3. Boundary-layer parameters

The mean velocity of the uniform shear flow is given by

$$U_1 = U_w + \lambda y,$$

where  $U_w$  can be referred to as the 'slip velocity' at the wall. The edge of the boundary layer  $y = \delta$  is assumed to be the position where  $U - U_1 = 0.005U_1$ . As this definition is somewhat arbitrary, it is desirable to introduce more reliably determined integral thicknesses to characterize the boundary layer.

The displacement thickness  $\delta^*$  is arbitrarily defined such that

$$\int_0^{\delta^*} U_1 dy = \int_0^{\infty} (U_1 - U) dy.$$

Thus

$$\frac{\delta^*}{\delta} + \frac{\lambda\delta}{2U_w} \left(\frac{\delta^*}{\delta}\right)^2 = \int_0^1 \left(\frac{U_1 - U}{U_w}\right) d(y/\delta). \quad (1)$$

In the present experiments, the parameters  $\lambda$ ,  $\delta$  and  $U_w$  are equal to  $6 \text{ s}^{-1}$ ,  $0.51 \text{ m}$  and  $4.9 \text{ ms}^{-1}$  respectively, so that  $\lambda\delta/U_w \simeq \frac{1}{16}$ . In the experiment of Masuda *et al.* (1972),  $\lambda = 60 \text{ s}^{-1}$ ,  $\delta = 0.0205 \text{ m}$  and  $U_w = 35 \text{ ms}^{-1}$ , so that  $\lambda\delta/U_w \simeq \frac{1}{28}$ . So, without significant loss of accuracy,

$$\frac{\delta^*}{\delta} = \int_0^1 \frac{U_1 - U}{U_w} d(y/\delta). \tag{2}$$

Only when  $\lambda\delta/U_w$  is  $O(1)$  is it necessary to use equation (1) for  $\delta^*$ .

The momentum thickness  $\Theta$  can be defined by

$$\int_0^\Theta U_1^2 dy = \int_0^\delta U_1(U_1 - U) dy,$$

which leads to

$$\frac{\Theta}{\delta} + \frac{\lambda\delta}{U_w} \left(\frac{\Theta}{\delta}\right)^2 + \frac{1}{3} \left(\frac{\lambda\delta}{U_w}\right)^2 \left(\frac{\Theta}{\delta}\right)^3 = \int_0^1 \frac{U}{U_w} \left(\frac{U_1 - U}{U_w}\right) d(y/\delta). \tag{3}$$

So, to the same order of accuracy as that implied by (2), we have

$$\frac{\Theta}{\delta} = \int_0^1 \frac{U}{U_w} \left(\frac{U_1 - U}{U_w}\right) d(y/\delta). \tag{4}$$

When  $\lambda = 0$ ,  $U_w = U_1$  and (2) and (4) are then the usual definitions of  $\delta^*$  and  $\Theta$  for a uniform external stream. Another suitable integral length parameter is  $\Delta$  (Clauser 1954), defined here as

$$\Delta = \int_0^\infty \frac{U_1 - U}{U_\tau} dy.$$

The momentum integral equation can be obtained by integrating the equation of motion

$$U \frac{\partial U}{\partial x} + V \frac{\partial U}{\partial y} = \frac{\partial \tau}{\partial y} \tag{5}$$

from  $y = 0$  to  $y = \delta$ . The integration, when combined with (4), yields

$$\frac{\partial \Theta}{\partial x} + \frac{\lambda}{U_w^2} \int_0^\delta \left(\frac{\partial U}{\partial x}\right) (\delta - y) dy = \frac{\tau_w - \tau_\delta}{U_w^2}. \tag{6}$$

The second term on the left-hand side is of order  $(\lambda\delta/U_w)(\delta/x)$  whilst

$$d\Theta/dx = O(\delta/x).$$

A reasonable approximation to the momentum integral equation is therefore

$$(\tau_w - \tau_1)/U_w^2 = d\Theta/dx,$$

or

$$c_f - c_{f1} = 2d\Theta/dx', \tag{7}$$

where  $\tau_\delta \simeq \tau_1$  and  $c_{f1} (= 2\tau_1/U_w^2)$  can be interpreted as an effective skin-friction coefficient for the external stream.

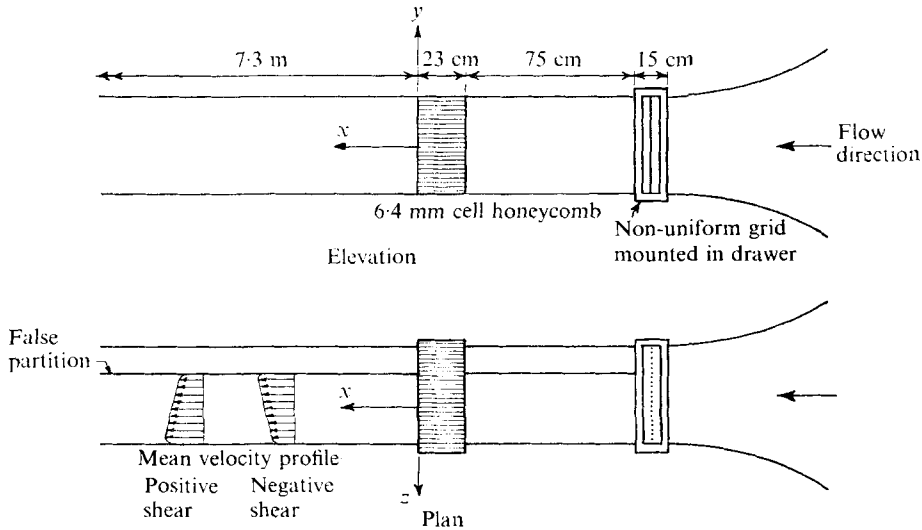


FIGURE 2. Schematic layout of shear-flow generator in wind tunnel.

#### 4. Experimental equipment and procedure

The open-return blower wind tunnel used for this investigation has a 9:1 contraction ratio and a 7.3 m long, 45.7 cm square working section. A non-uniform grid shear-flow generator is inserted in a drawer at the end of the contraction and a uniform 23 cm deep  $\times$  6.4 mm hexagonal-cell aluminium honeycomb is placed 76.2 cm downstream from the shear-flow generator.† The main purpose of the honeycomb is to remove the lateral gradients in turbulence length scale which persist behind the non-uniform grid. The spacing of the bars in the grid is adjusted by trial and error to obtain a positive uniform mean shear with a gradient  $\lambda$  of approximately  $6 \text{ s}^{-1}$  downstream of the honeycomb. Another grid, in which the spacing between bars is exactly the reverse of that in the first grid (i.e. the larger spacing between the generator bars, corresponding to the high-speed side of the uniform shear flow, is now near the false wall), generates a uniform shear flow with a velocity gradient  $\lambda$  equal to  $-6 \text{ s}^{-1}$ . A third, empty drawer is inserted in place of the generator when a uniform flow with zero velocity gradient is required.

A schematic diagram of the working-section arrangement is given in figure 2. In the co-ordinate system used,  $x$  is the longitudinal distance measured from the honeycomb,  $y$  is the distance normal to the false partition and  $z$  is measured in the plane of the partition. The mean velocity components in the  $x$ ,  $y$  and  $z$  directions are  $U$ ,  $V$  and  $W$  respectively whilst the corresponding velocity fluctuations are  $u$ ,  $v$  and  $w$ . The boundary layer studied in this paper develops along the false partition and its virtual origin is stabilized by a 1.6 mm diameter rod situated at  $x = 23 \text{ cm}$ .

† A more complete description of the wind tunnel, shear-flow generator and traverse gear may be found in Mulhearn & Luxton (1970).

Mean velocity measurements are made with both a Pitot tube and a single normal hot wire (for details, see Ahmad, Luxton & Antonia 1975*b*).

The mean kinematic Reynolds shear stress is obtained with a single inclined hot wire operated with a linearized constant-temperature anemometer system (DISA 55D01, 55D15). The stress  $-\overline{uv}$  is proportional to the difference between the two mean-squared values of the linearizer fluctuating voltages obtained before and after a 180° rotation of the wire. The stress  $-\overline{uv}$  can also be obtained with an X-wire but this is primarily used to measure  $w$  fluctuations and the Reynolds stresses  $-\overline{uw}$  and  $-\overline{vw}$  as  $-\overline{uv}$  tends to extrapolate to wall stress values which are lower than those found by other methods. The linearized signals from the X-wire are fed into a multiplying and adding circuit from which the instantaneous  $u$ ,  $v$  (or  $w$ ) and  $uv$  (or  $uw$ ) signals are recorded on a Hewlett-Packard 3525A 7-channel FM tape recorder at a speed of 38.1 cm s<sup>-1</sup> (the frequency response of the tape recorder is flat up to 5 kHz). The records are typically of 20 s duration. Spectra of  $u$ ,  $v$  and  $w$  may be obtained by playing back the recorded signals through a series of bandpass filters of the DISA 55D26 signal conditioner and recording the r.m.s. output from the 55D35 voltmeter.

## 5. Mean velocity profile data

The experimental mean velocity profiles are plotted in the form  $U/U_\tau$  vs.  $\log yU_\tau/\nu$ , where the values of the friction velocity  $U_\tau$  ( $\equiv \tau_w^{1/2}$ , where  $\tau_w$  is the kinematic wall stress) are determined by the Preston-tube method (with the calibration of Head & Ram 1971). These values are in close agreement with those obtained from the Clauser chart and the inclined-wire measurements near the wall. The profiles are shown in figure 3 for  $\lambda = \pm 6$  s<sup>-1</sup> respectively. At each value of  $\lambda$ , profiles are shown for three values of  $x$  (1.37, 1.63 and 2.21 m). The viscous-sublayer relation  $U/U_\tau = yU_\tau/\nu$  appears to be closely followed up to a value of  $yU_\tau/\nu \simeq 10$ . For  $yU_\tau/\nu > 30$ , the profiles conform with the logarithmic relation

$$\frac{U}{U_\tau} = \frac{1}{K} \log \frac{yU_\tau}{\nu} + C, \quad (8)$$

with  $K \simeq 0.40$  and  $C = 5.0$ , the values recommended by Coles (1962) in his appraisal of turbulent boundary layers with small external turbulence levels. The region of validity of (8) appears to be narrower in the presence of an external shear flow than when the flow field is uniform. For  $\lambda = \pm 6$  s<sup>-1</sup>, (8) is valid up to  $yU_\tau/\nu = 120$  and 250 respectively whilst with  $\lambda = 0$ , the validity extends up to  $yU_\tau/\nu = 300$ . It should be noted however that the values of  $R_\Theta$ , defined as  $U_\delta \Theta/\nu$  ( $U_\delta$  is the velocity at  $y = \delta$ , equal to  $U_w \pm \lambda\delta$ ), are sufficiently different to account for the above differences in the extent of relation (8). The mean velocity profiles of Charnay, Comte-Bellot & Mathieu (1972) show a significant shift to higher values than those given by (8) (with  $K = 0.41$  and  $C = 5.7$ ) when  $T_u = 4.7\%$ , but a straight-line portion on a semi-logarithmic plot still exists. Kline, Lisin & Waitman (1960) also observed a departure from (8) for  $T_u > 4\%$  but, in their case, the values of  $U/U_\tau$  in the logarithmic region are below those given by (8) (with  $K = 0.47$  and  $C = 5.2$ ).

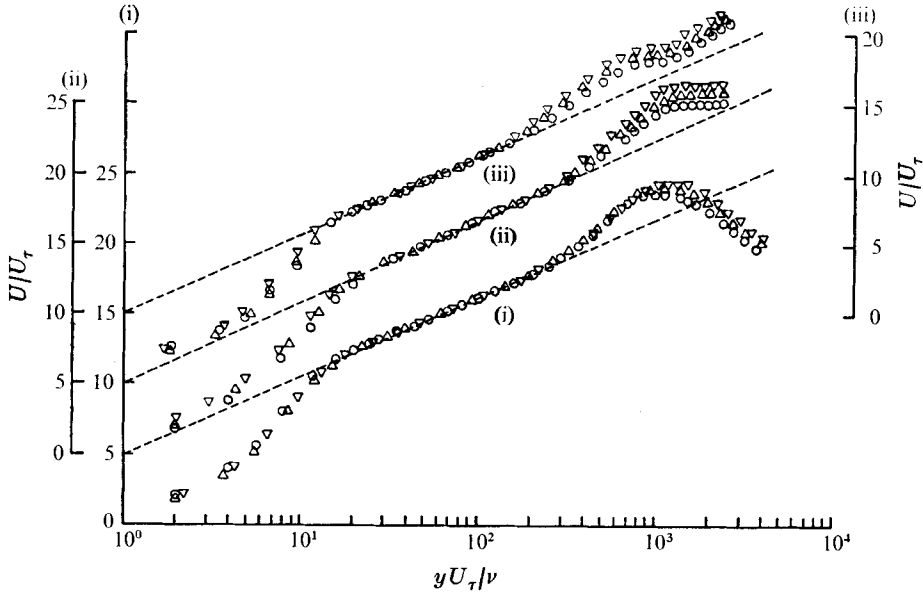


FIGURE 3. Mean velocity profiles. (i)  $\lambda = -6 \text{ s}^{-1}$ , (ii)  $\lambda = 0$ , (iii)  $\lambda = 6 \text{ s}^{-1}$ .  
Three stations:  $\circ$ , 1.37 m;  $\triangle$ , 1.63 m;  $\nabla$ , 2.21 m.

In the outer region of the layer, the velocity profiles are different for different  $x$  since no collapse is expected when the normalizing length scale  $\nu/U_\tau$  is used. The increase in values of  $U/U_\tau$  with increasing  $x$  reflects the decrease in the wall stress with downstream distance. In the case of an external shear flow, the profiles merge into the profiles  $U_1/U_\tau = U_w/U_\tau \pm |\lambda| yU_\tau/\nu$ , but before the merging occurs a small zone exists where  $U$  is approximately constant. The extent of this zone is about the same when  $\lambda = -6 \text{ s}^{-1}$ . This region is not apparent in the measurements of Masuda *et al.* (1972) for  $\lambda = \pm 60 \text{ s}^{-1}$ , but it is observed on some of the profiles measured by Costin (1971) for  $\lambda = 15 \text{ s}^{-1}$ . No other writers have published data close enough to the boundary to determine whether a plateau region existed in their experiments. Although we do not yet have a plausible explanation for the plateaux, measurements of turbulence quantities presented in §6 are consistent with such plateaux of  $U$  near the outer 'edge' of the layer. Tentatively one may suggest that the plateaux will probably exist at low  $\lambda$  because of the efficient large-scale mixing and entrainment in the outer region of the boundary layer, which destroys the mean shear of the external flow. At large  $\lambda$  however, the external shear flow may dominate and inhibit the large-scale mixing and entrainment in the outer part of the boundary layer, thus accounting for the disappearance of the plateaux. Masuda *et al.* (1972), as pointed out earlier, did not find a plateau region for  $\lambda = \pm 60 \text{ s}^{-1}$  but did find marked changes in the structure of the outer region of the boundary layer, which is consistent with the above postulate, provided their results are reliable.

Before discussing the mean velocity profiles in the outer region of the layer in more detail, it seems appropriate here to investigate the possibility of self-

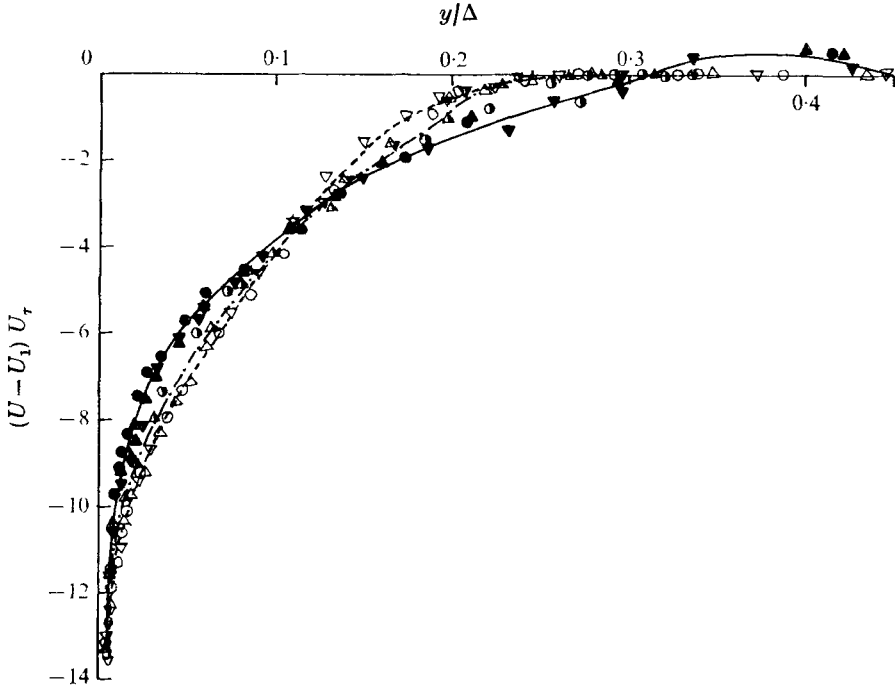


FIGURE 4. Velocity defect profiles for three external shears at three stations. Zero external shear:  $\bullet$ , 1.37 m;  $\blacktriangle$ , 1.63 m;  $\blacktriangledown$ , 2.21 m. Positive external shear:  $\bullet$ , 1.37 m;  $\blacktriangle$ , 1.63 m;  $\blacktriangledown$ , 2.21 m. Negative external shear:  $\circ$ , 1.37 m;  $\triangle$ , 1.63 m;  $\triangledown$ , 2.21 m.

preservation for a turbulent boundary layer with an external uniform shear flow. In the case of small  $\lambda$ , it is reasonable to seek self-preserving solutions of the equations of motion for the departures of the mean velocity and Reynolds-stress distributions from those associated with the external uniform shear flow. Excluding the region of the flow in the immediate vicinity of the wall that is directly affected by viscosity, we seek self-preserving solutions of the form<sup>†</sup>

$$U_1 - U = U_0 f(y/\delta_0, \lambda\delta_0/U_w, (\overline{u_1^2})^{1/2}/U_w), \tag{9}$$

$$\left. \begin{aligned} \overline{u_1^2} - \overline{u^2} &= U_0^2 g_1(y/\delta_0, \lambda\delta_0/U_w, (\overline{u_1^2})^{1/2}/U_w), \\ \overline{v_1^2} - \overline{v^2} &= U_0^2 g_2(y/\delta_0, \lambda\delta_0/U_w, (\overline{u_1^2})^{1/2}/U_w), \\ (\overline{uv})_1 - \overline{uv} &= U_0^2 g_{12}(y/\delta_0, \lambda\delta_0/U_w, (\overline{u_1^2})^{1/2}/U_w), \end{aligned} \right\} \tag{10}$$

where  $U_0$  and  $\delta_0$  are the velocity and length scales respectively and the functions  $f$ ,  $g_1$ ,  $g_2$  and  $g_{12}$  are presumably universal functions of  $y/\delta_0$ ,  $\lambda\delta_0/U_w$  and the

<sup>†</sup> This approach is somewhat similar to that used by Townsend (1965, 1966), who postulated self-preservation of the perturbation to a boundary layer subjected to sudden changes in surface conditions. It should be noted here that the form of self-preservation proposed for the difference in Reynolds stresses is probably only applicable to the case of small  $T_u$  as we are implicitly assuming that the turbulence field associated with the boundary layer is uncorrelated with that due to the free stream.

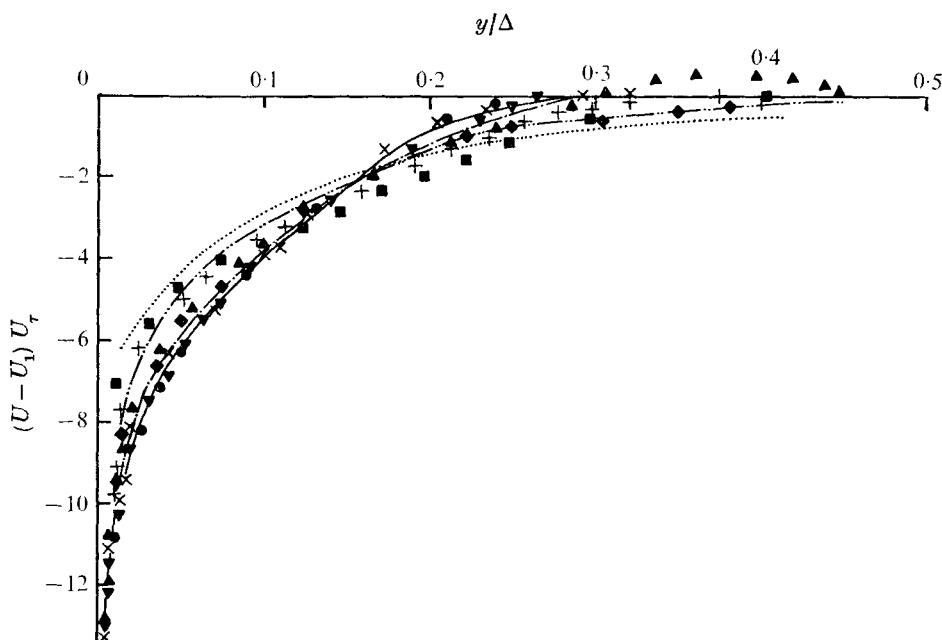


FIGURE 5. Velocity defect profiles for different external turbulence levels  $T_u$  and for different external shears  $\lambda$ . —, Clauser (1956),  $T_u = 0.2\%$ ,  $\lambda = 0$ ; ●, Antonia (1969),  $T_u = 0.2\%$ ,  $\lambda = 0$ ; ·····, Kline *et al.* (1960),  $T_u = 6.2\%$ ,  $\lambda = 0$ . Charnay *et al.* (1972): ×,  $T_u = 0.3\%$ ,  $\lambda = 0$ ; — · — · — · —,  $T_u = 4.7\%$ ,  $\lambda = 0$ . Masuda *et al.* (1972): ◆,  $T_u = 2.8\%$ ,  $\lambda = -60 \text{ s}^{-1}$ ; ■,  $T_u = 3.4\%$ ,  $\lambda = +60 \text{ s}^{-1}$ ; +,  $T_u = 3.6\%$ ,  $\lambda = 0$ . Present results: ▼,  $T_u = 1.6\%$ ,  $\lambda = -6 \text{ s}^{-1}$ ; — · —,  $T_u = 1.5\%$ ,  $\lambda = 0$ ; ▲,  $T_u = 1.3\%$ ,  $\lambda = 6 \text{ s}^{-1}$ .

external-flow turbulence level.† The stresses  $\overline{u_1^2}$ ,  $\overline{v_1^2}$  and  $-(\overline{uv})_1$  do not depend on  $y$  in the case of a uniform shear flow. Substitution of (9) and (10) into the equation of motion and use of the continuity equation leads to requirements on the streamwise development of  $U_0$  and  $\delta_0$  that are identical to those obtained by Townsend (1956, p. 231, 1966) for the corresponding situation of a turbulent boundary layer developing with zero pressure gradient and a uniform external free stream with a low turbulence level. It must be emphasized that in our case  $(\overline{uv})_1$  is only a small fraction of the wall stress (about 10%), so that we presume that we are investigating a small perturbation by the external shear flow on the boundary layer. A suitable choice for the velocity scale  $U_0$  is  $U_\tau$  since, in the inner region of the flow, (9) is consistent with the experimentally observed logarithmic relation (8). For the length scale  $\delta_0$ , we choose the integral thickness  $\Delta$ .

Velocity profiles are shown in figure 4 in the form  $(U - U_1)/U_\tau$  vs.  $y/\Delta$  for the three values of  $\lambda$ . The agreement of the data with (9) is good and the data for each value of  $\lambda$  can be represented by a single curve, shown in figure 5 for comparison with other experimental data. The profiles for low free-stream turbulence

† It is of course possible that the functions  $f$ ,  $g_1$ ,  $g_2$  and  $g_{12}$  also depend on other characteristics of the external shear-flow turbulence, e.g. the turbulence length scale. The limited experimental evidence available suggests that, at least in the case of  $f$ , this dependence is likely to be negligible.

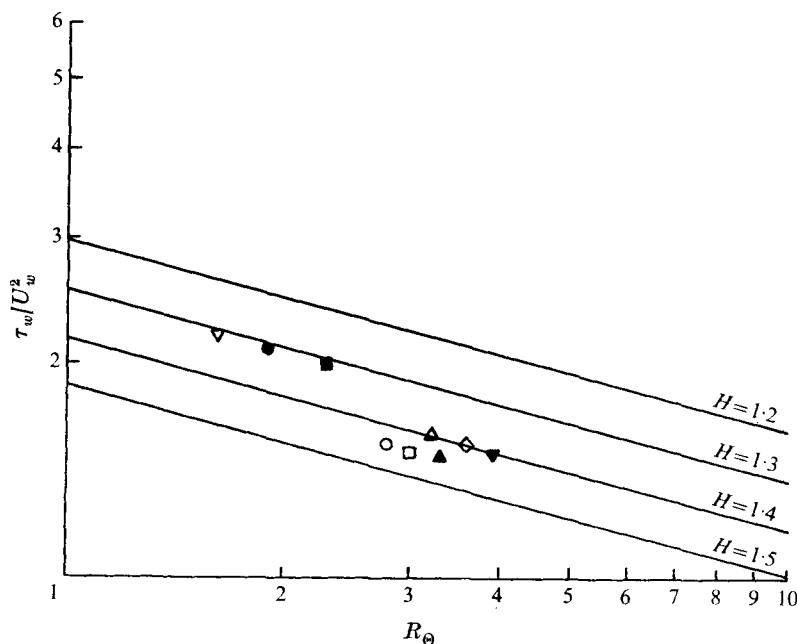


FIGURE 6. Turbulent shearing stress at the wall. Positive external shear ( $T_u = 1.3\%$ ):  $\nabla$ ,  $H = 1.42$ ,  $x = 1.37$  m;  $\bullet$ ,  $H = 1.37$ ,  $x = 1.63$  m;  $\blacksquare$ ,  $H = 1.29$ ,  $x = 2.21$  m. Zero external shear ( $T_u = 1.5\%$ ):  $\triangle$ ,  $H = 1.36$ ,  $x = 1.37$  m;  $\diamond$ ,  $H = 1.35$ ,  $x = 1.63$  m;  $\blacktriangledown$ ,  $H = 1.38$ ,  $x = 2.21$  m. Negative external shear ( $T_u = 1.6\%$ ):  $\circ$ ,  $H = 1.37$ ,  $x = 1.37$  m;  $\square$ ,  $H = 1.40$ ,  $x = 1.63$  m;  $\blacktriangle$ ,  $H = 1.46$ ,  $x = 2.21$  m; —, Ludwig & Tillman equation.

of Charnay *et al.* (1972) and Antonia (1969) are in good agreement with Clauser's (1956) profile. As the external turbulence level increases, the magnitude of  $|U - U_1|/U_\tau$  decreases in the inner part of the layer. This decrease is brought about by the increase in  $U_\tau$  (Kline *et al.* 1960; Charnay *et al.* 1972) as  $(\overline{u_1^2})^{1/2}$  is increased. For  $y/\Delta > 0.16$ , the defect  $|U - U_1|/U_\tau$  now increases as  $T_u$  increases with respect to the 'asymptotic' Clauser profile. It should be recalled here that the area under the experimental curves in figure 5 is constrained to be unity [equation (2)]. The present data for  $\lambda = 0$  ( $T_u = 1.5\%$ ) are consistent with the trend of the data of Charnay *et al.* (1972). The data points of  $|U - U_1|/U_\tau$  for  $\lambda = +6 \text{ s}^{-1}$  are also consistent with this trend. For  $y/\Delta > 0.3$ , the values for  $\lambda = +6 \text{ s}^{-1}$  exhibit a region where  $U$  exceeds  $U_1$ , which is a consequence of the observed plateau in  $U$  near the outer edge of the layer. Surprisingly, the data for  $\lambda = -6 \text{ s}^{-1}$  follow the Clauser curve fairly closely even though  $T_u$  for  $\lambda = -6 \text{ s}^{-1}$  (1.6%) is slightly greater than for  $\lambda = 0$  (1.5%). Masuda *et al.* (1972) concluded from their data with fairly high  $\lambda$  ( $\pm 60 \text{ s}^{-1}$ ) that the position of their data on the defect plot  $(U_1 - U)/U_\tau$  vs.  $y/\Delta$  was determined uniquely by the turbulence level  $T_u$  and that the shear did not apparently exert any additional influence. A close examination of the data of Masuda *et al.* in figure 6 reveals however that, for  $\lambda = +60 \text{ s}^{-1}$ , the values of  $|U - U_1|/U_\tau$  near the wall are significantly lower than those for  $\lambda = 0$  and a slightly higher level of  $T_u$ .

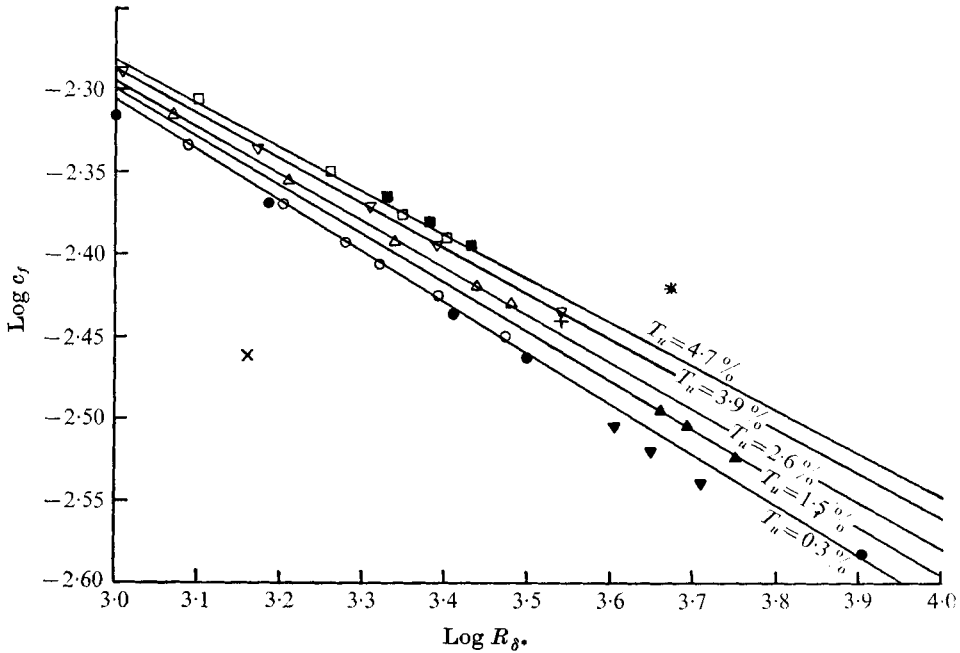


FIGURE 7. Relation between skin-friction coefficient  $c_f$  and Reynolds number  $R_{\delta^*}$ . Charnay *et al.* (1972) ( $\lambda = 0$ ):  $\circ$ ,  $T_u = 0.3\%$ ;  $\triangle$ ,  $T_u = 2.6\%$ ;  $\nabla$ ,  $T_u = 3.9\%$ ;  $\square$ ,  $T_u = 4.7\%$ . Masuda *et al.* (1972):  $\times$ ,  $\lambda = -60 \text{ s}^{-1}$ ,  $T_u = 2.8\%$ ;  $*$ ,  $\lambda = +60 \text{ s}^{-1}$ ,  $T_u = 3.4\%$ ;  $+$ ,  $\lambda = 0$ ,  $T_u = 3.6\%$ . Present results:  $\blacksquare$ ,  $\lambda = +6 \text{ s}^{-1}$ ,  $T_u = 1.3\%$ ;  $\blacktriangle$ ,  $\lambda = 0$ ,  $T_u = 1.5\%$ ;  $\blacktriangledown$ ,  $\lambda = -6 \text{ s}^{-1}$ ,  $T_u = 1.6\%$ ;  $\bullet$ , Wood (1975),  $\lambda = 0$ ,  $T_u \simeq 0.2\%$ . —,  $c_f = c_{f0}(\frac{1}{31.8}R_{\delta^*})^{T_u}$ .

The trend of the present data and the data of Masuda *et al.*† would seem to be more consistent with a larger increase in  $U_r$  when  $\lambda$  is positive and with a decrease when  $\lambda$  is negative.

The plot of  $\tau_w/U_w^2 (= \frac{1}{2}c_f)$ , where  $c_f$  is the skin-friction coefficient) *vs.*  $R_\Theta (= U_w\Theta/\nu)$  in figure 6 shows that the Ludwig & Tillman relation does not adequately represent the data when there is a non-negligible external turbulence level. It is useful therefore to establish an empirical relation between  $c_f$ ,  $H$ ,  $R_\Theta$  and  $T_u$  for such a case. Bradshaw (1974), following Green's (1972) analysis, obtained a relation for the skin-friction coefficient  $c_f$  (for  $T_u < 5\%$ ):

$$c_f = c_{f0}(1 + AT_u),$$

where  $c_{f0}$  is the skin-friction coefficient for a non-turbulent stream at the same  $R_\Theta$  and  $A$  was assumed by Bradshaw to be a universal constant equal to 3.2. However, if  $A$  is evaluated from the experimental data (Charnay *et al.* 1972; Huffman, Zimmerman & Bennet (1972) and the present results), it is found to vary from 1.5 to 4.6 for  $2000 < R_\Theta < 8000$ . The value of  $A$  obtained from figure 12 of Charnay's (1974) thesis is 4.4. Figure 7 shows a systematic increase in  $c_f$

† It should be pointed out that the data of Masuda *et al.* may have suffered from the problems associated with the open jet configuration in their experimental arrangement. Also, the shear-flow generating grid upstream from the flat plate imposes a non-uniform length-scale distribution in the direction of the shear flow.

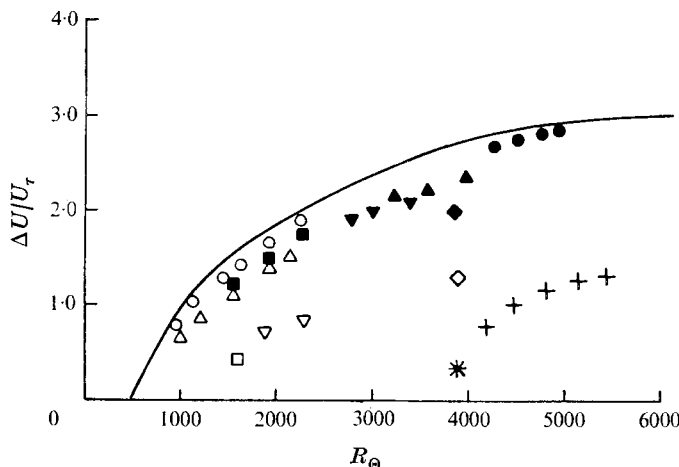


FIGURE 8. Relation between maximum defect  $\Delta U/U_\tau$  and Reynolds number  $R_\Theta$ . Charnay *et al.* (1972) ( $\lambda = 0$ ): symbols same as for figure 6. Huffman *et al.* (1972) ( $\lambda = 0$ ): ●,  $T_u = 0.1\%$ ; +,  $T_u = 3.1\%$ . Kline *et al.* (1960) ( $\lambda = 0$ ): ◆,  $T_u = 2.2\%$ ; ◇,  $T_u = 3.6\%$ ; \*,  $T_u = 6.4\%$ . Present results: symbols same as for figure 6. —, Coles (1962),  $\lambda = 0$ ,  $T_u \approx 0.2\%$ .

as  $T_u$  increases, at a given value of  $R_{\delta^*}$ . Our values of  $c_f$  and those of Masuda *et al.* (1972) for  $\lambda = 0$  appear to agree with the trend of the data of Charnay *et al.*, their position in figure 7 corresponding to the appropriate  $T_u$ . A good fit to these data is given by the empirical relation  $c_f = c_{f0}(\frac{1}{31.6} R_{\delta^*})$  in the range

$$1000 < R_{\delta^*} < 8000,$$

but it remains to be seen whether  $A$  continues to depend on the Reynolds number when the velocity defect law ceases to do so (see figure 8). It is clear from figure 7 that the values of  $c_f$  for  $\lambda \neq 0$  do not follow the same pattern as those for  $\lambda = 0$ . When  $\lambda > 0$ ,  $c_f$  is significantly higher than the value corresponding to  $\lambda = 0$  for the same value of  $T_u$ , whilst for  $\lambda < 0$ ,  $c_f$  is greatly reduced with respect to its  $\lambda = 0$  value.

To investigate the effects of the external turbulence level, the maximum defect normalized with friction velocity  $\Delta U/U_\tau$  is plotted against  $R_\Theta$  in figure 8 for different turbulence levels with and without external shear. The turbulence level  $T_u$  ranges from the negligible values considered by Coles (1962) to about 6.4% (Kline *et al.* 1960). It is observed that the effect of increasing the turbulence level is to decrease the strength of the 'wake' component and hence to increase the local friction coefficient at a fixed Reynolds number. From the log-law equation  $\Delta U/U_\tau$  is related to  $R_\Theta$  by the equation

$$\frac{\Delta U}{U_\tau} = \frac{2}{c_f} + \frac{\lambda \delta}{U_\tau} - \frac{1}{K} \log \left\{ \frac{\delta}{\Theta} \left( \frac{c_f}{2} \right)^{\frac{1}{2}} \right\} - C - \frac{1}{K} \log R_\Theta. \quad (11)$$

Figure 9 shows that the quantity  $\Delta U/U_\tau$  becomes quite low, being reduced to less than one fifth of its low turbulence value for a turbulence level of 6.4%.

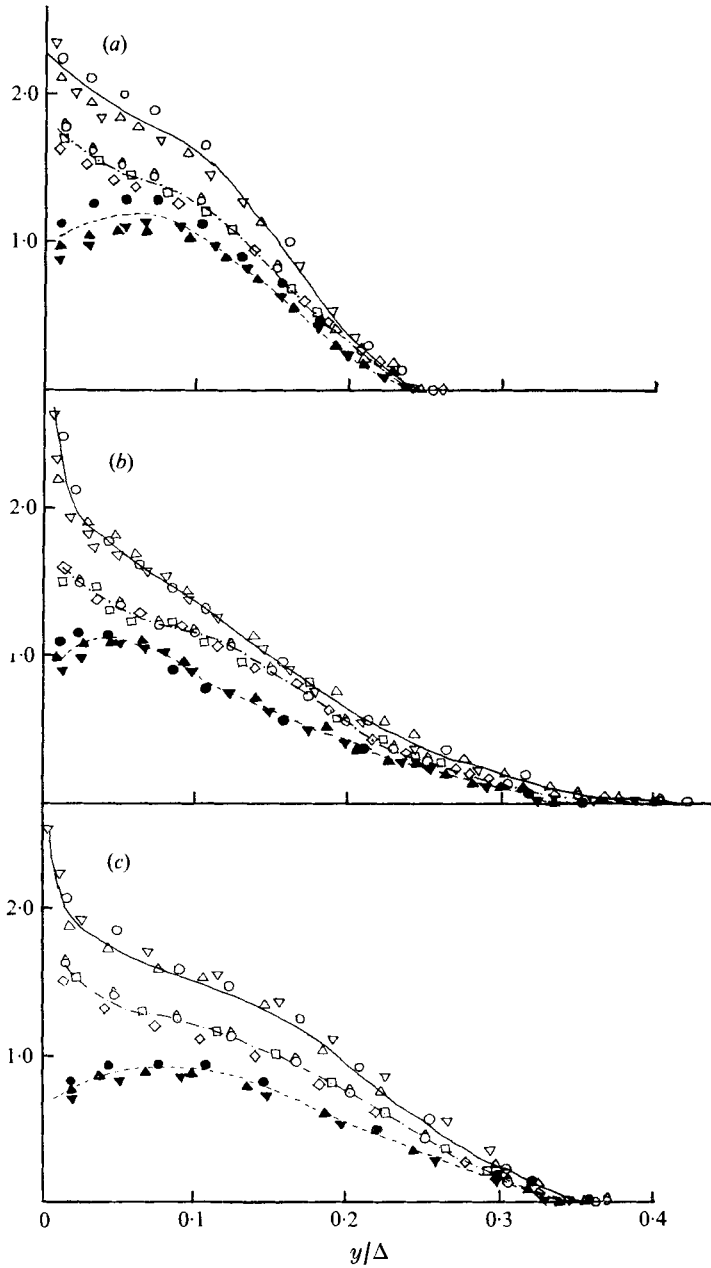


FIGURE 9. Distribution of turbulence intensities for (a)  $\lambda = 6 \text{ s}^{-1}$ , (b)  $\lambda = 0$  and (c)  $\lambda = -6 \text{ s}^{-1}$ .  $(\overline{u^2} - \overline{u_1^2})^{1/2}/U_\tau$ :  $\circ$ ,  $x = 1.37 \text{ m}$ ;  $\triangle$ ,  $x = 1.63 \text{ m}$ ;  $\nabla$ ,  $x = 2.21 \text{ m}$ .  $(\overline{v^2} - \overline{v_1^2})^{1/2}/U_\tau$ :  $\bullet$ ,  $x = 1.36 \text{ m}$ ;  $\blacktriangle$ ,  $x = 1.63 \text{ m}$ ;  $\blacktriangledown$ ,  $x = 2.21 \text{ m}$ .  $(\overline{w^2} - \overline{w_1^2})^{1/2}/U_\tau$ :  $\circ$ ,  $x = 1.37 \text{ m}$ ;  $\diamond$ ,  $x = 1.63 \text{ m}$ ;  $\square$ ,  $x = 2.21 \text{ m}$ .

It is found that, at constant  $R_\theta$ ,  $\Delta U/U_\tau$  is well approximated (for  $T_u > 1\%$ ) by the relation

$$\Delta U/U_\tau = 3.56 - 3 \left( \frac{2}{c_f} \right)^{\frac{1}{2}} T_u, \quad (12)$$

which supports Bradshaw's (1974) assumption that  $(\pi - \pi_0) \propto (2/c_f)^{\frac{1}{2}} T_u$  in the case of zero shear†  $\pi$  and  $\pi_0$  being the 'wake' strengths for a turbulent and non-turbulent external flow respectively. The calculated values of the boundary-layer parameters are presented in table 1.

## 6. Turbulence data

### 6.1. Reynolds normal stresses

The measured distributions of  $(\overline{u^2})^{\frac{1}{2}}/U_w$  and  $-\overline{uv}/\tau_w$  for  $\lambda = 0$  compare favourably with the results of Charnay *et al.* (1972), which clearly indicate that both  $\overline{u^2}$  and  $-\overline{uv}$  increase appreciably with an increase in  $T_u$  in the outer layer.

Distributions of  $(\overline{u^2} - \overline{u_1^2})^{\frac{1}{2}}/U_\tau$ ,  $(\overline{v^2} - \overline{v_1^2})^{\frac{1}{2}}/U_\tau$  and  $(\overline{w^2} - \overline{w_1^2})^{\frac{1}{2}}/U_\tau$  plotted against  $y/\Delta$  are shown in figure 9 for the present three values of  $\lambda$ . The results seem to support, at least qualitatively, the concept of self-preservation outlined in §5 and most of the data at three streamwise stations can be adequately represented by a single distribution.‡ The distributions of  $(\overline{u^2} - \overline{u_1^2})^{\frac{1}{2}}/U_\tau$  for the three values of  $\lambda$  are replotted in figure 10 together with those of Klebanoff (1954) for  $T_u \simeq 0.2\%$  and those of Charnay *et al.* (1972) for  $T_u = 0.3\%$  and  $4.7\%$ . The values of Charnay *et al.* for  $T_u = 0.3\%$  seem to be rather high compared with those of Klebanoff (1954) ( $T_u = 0.2\%$ ), which may be due to the difference in initial conditions between the two cases. The distribution for  $\lambda = -6 \text{ s}^{-1}$  is appreciably lower than that for  $\lambda = 0$  in the outer region ( $y/\Delta > 0.15$ ) of the layer whereas the distribution for  $\lambda = +6 \text{ s}^{-1}$  lies above that for  $\lambda = 0$ . For  $y/\Delta < 0.15$ , the distribution for  $\lambda = -6 \text{ s}^{-1}$  is higher than that corresponding to  $\lambda = 0$  or  $\lambda = +6 \text{ s}^{-1}$ . This trend is also apparent from the distribution of  $(\overline{v^2} - \overline{v_1^2})^{\frac{1}{2}}/U_\tau$  in figure 10. This means that with external shear, due to variation in the free-stream velocity  $U_1$ , the outer boundary condition on the turbulent energy equation varies and this perturbation propagates inwards with the increase and decrease in  $\overline{q^2}$  for positive and negative shear respectively.

† Charnay *et al.* (1972) collapsed their velocity defect profiles by plotting

$$(U_1 - U)/[U_\tau - \alpha(\overline{u_1^2})^{\frac{1}{2}}]$$

as a function of  $y/\delta$  with  $\alpha \simeq \frac{1}{3}$ . There does not seem to be any physical justification for choosing  $U_\tau - \alpha(\overline{u_1^2})^{\frac{1}{2}}$  as the appropriate velocity scale. Also, the implication that the value of  $K$  in the log-law region varies with  $T_u$  is not in agreement with the experimental results. Further, as Bradshaw (1974) has already commented, the choice of the length scale  $\delta$  is rather critical.

‡ Gorlin & Zrazhskii (1972) found that, in a boundary layer with different surface roughness conditions and different values of  $T_u$ , the quantity

$$V = [(\overline{u^2})^{\frac{1}{2}} - (\overline{u_1^2})^{\frac{1}{2}}]/[(\overline{u_{\max}^2})^{\frac{1}{2}} - (\overline{u_1^2})^{\frac{1}{2}}]$$

is a linear function of  $y/\delta_*$ , where  $\delta_* = \int_0^\infty V dy$ . The interpretation of this result is somewhat obscured by the difficulty of interpreting  $\delta_*$ .

External shear $\lambda$ ( $s^{-1}$ )	$T_u$ (%)	$x$ (m)	$U_w$ ( $ms^{-1}$ )	$U_1$ ( $ms^{-1}$ )	$U_T$ ( $ms^{-1}$ )	$c_f$ †	$\Delta$ (mm)	$\delta'$ (mm)	$\delta$ (mm)	$\delta^*$ (mm)	$\Theta$ (mm)	$H$	$\left(\frac{\Delta U}{U_T}\right)_{max}$	$U_w \Theta / \nu$	$U_w \delta / \nu$	$U_w \delta^* / \nu$
+6	1.3	1.37	4.88	5.23	0.229	0.0044	111.3	40.6	66.0	6.50	4.57	1.42	1.61	1500	19200	2130
		1.63	4.88	5.29	0.223	0.0042	114.3	50.8	73.7	7.32	5.33	1.37	1.75	1750	22500	2400
		2.21	4.88	5.36	0.218	0.0040	117.6	61.0	81.3	8.20	6.35	1.29	2.12	2670	26700	2690
-6	1.6	1.37	6.40	6.04	0.253	0.0031	240.0	38.1	61.0	9.42	6.86	1.37	2.18	2970	26300	4060
		1.63	6.40	6.00	0.247	0.0030	266.7	43.2	66.0	10.29	7.37	1.40	2.22	3200	28400	4430
		2.21	6.40	5.96	0.244	0.0029	311.2	50.8	73.7	11.84	8.13	1.46	2.30	3550	31700	5100
0	1.5	1.37	6.71	6.71	0.268	0.0032	241.3	63.5	63.5	9.65	7.11	1.36	2.15	3200	28600	4350
		1.63	6.71	6.71	0.262	0.0031	271.8	71.1	71.1	10.62	7.87	1.35	2.25	3550	32100	4790
		2.21	6.71	6.71	0.259	0.0030	317.5	76.2	76.2	12.27	8.89	1.38	2.35	3900	34400	5530

TABLE 1. Boundary-layer parameters.  $\delta'$  is the value of  $y$  at the start of the plateau ( $\partial U / \partial y = 0$ );  $\delta$  is the value of  $y$  at the end of the plateau ( $\partial U / \partial y = 0$ ); † Determined by Preston-tube method.

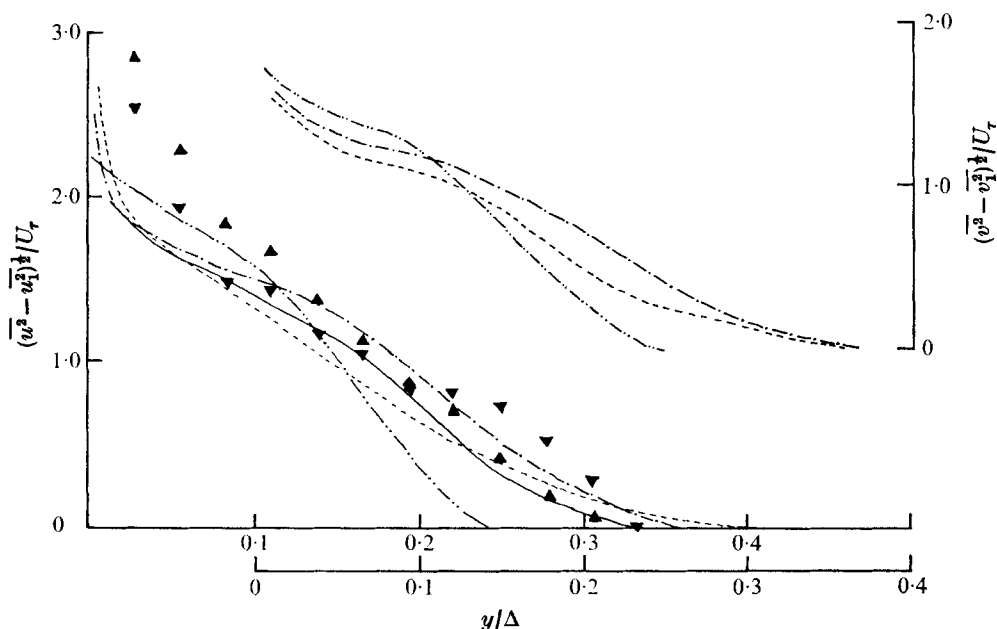


FIGURE 10. Distribution of longitudinal turbulence intensities for different external turbulence levels and external shears. Charnay *et al.* (1972) ( $\lambda = 0$ );  $\blacktriangle$ , 0.3%;  $\blacktriangledown$ , 4.7%. Present results: ---,  $\lambda = 0$ ,  $T_u = 1.5\%$ ; -·-,  $\lambda = +6 \text{ s}^{-1}$ ,  $T_u = 1.3\%$ ; ····,  $\lambda = -6 \text{ s}^{-1}$ ,  $T_u = 1.5\%$ . —, Klebanoff (1954),  $\lambda = 0$ ,  $T_u \approx 0.22\%$ .

### 6.2. Reynolds shear stress

The distributions of  $[(\overline{uv})_1 - \overline{uv}]/U_\tau^2$  for the three values of  $\lambda$  are shown in figure 11. Although the range of  $x$  is rather narrow, they tend to confirm the self-preserving nature of  $|\overline{uv} - \overline{uv}(\cdot)_1|$  throughout the layer. When  $\lambda > 0$ , the magnitude of the shear stress becomes negligible in that part of the outer layer characterized by the plateau in the mean velocity profile, and then increases (without a change in sign) to reach a constant value  $-(\overline{uv})_1$  appropriate to the external shear. For  $\lambda < 0$  the shear stress also becomes zero when  $\partial U/\partial y = 0$  but then changes its sign before finally attaining a constant value, equal to about one-third of the value of  $|(\overline{uv})_1|$  for  $\lambda > 0$ . As a result the distribution of  $[(\overline{uv})_1 - \overline{uv}]/U_\tau^2$  displays a negative region in the outer part of the layer for  $\lambda > 0$  but no such region is observed when  $\lambda < 0$  (figure 11).† In the region very near the wall ( $y/\Delta < 0.05$ ) the results are not appreciably affected by the external shear. The shear stress is however quite strongly influenced by the external shear in both the ‘log’ and the outer region of the layer. For  $\lambda > 0$ , there is a noticeable increase in the values of  $[(\overline{uv})_1 - \overline{uv}]/U_\tau^2$  in relation to those for  $\lambda = 0$ , whilst a large decrease is observed for  $\lambda < 0$ . This trend is in qualitative agreement with that displayed by the  $\overline{u^2} - \overline{u_1^2}$  and  $\overline{v^2} - \overline{v_1^2}$  data of figure 10 for  $y/\Delta$  greater than about 0.15. Charnay *et al.* (1972) and Huffman *et al.* (1972) have shown that increasing the turbulence

† The distributions of Reynolds shear stress of Ahmad, Luxton & Antonia (1975*a*) in a two-dimensional turbulent wake of a cylinder immersed in a uniform shear flow are consistent with these trends.

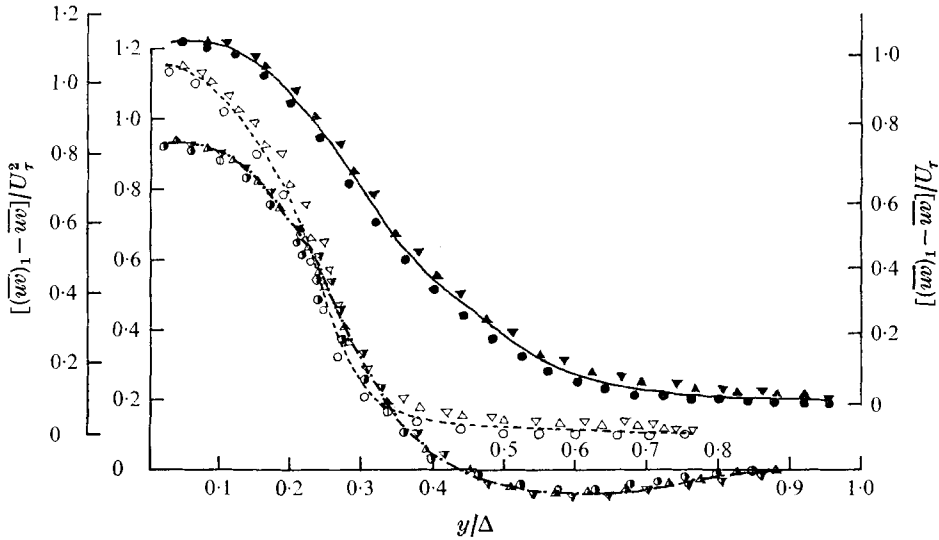


FIGURE 11. Lateral development of  $[(\overline{uv})_1 - \overline{uv}]/U_\tau^2$  for three external shears at three stations. Positive external shear:  $\bullet$ , 1.37 m;  $\blacktriangle$ , 1.63 m;  $\blacktriangledown$ , 2.21 m. Zero external shear:  $\bullet$ , 1.37 m;  $\blacktriangle$ , 2.63 m;  $\blacktriangledown$ , 2.21 m. Negative external shear:  $\circ$ , 1.37 m;  $\triangle$ , 1.63 m;  $\triangledown$ , 2.21 m.

level causes the shear stress to vanish at increasingly larger  $y/\Delta$ . According to Bradshaw (1974), this phenomenon may be the result of an increase in entrainment with increasing  $T_u$ . The major influence of the external mean shear or the outer layer is probably also through the entrainment.

### 6.3. Turbulent energy balance

The terms for the production, dissipation and advection of turbulent energy have been calculated and are presented in this subsection, normalized with  $U_\tau$  and  $\delta$  for all three values of  $\lambda$ . Advection was obtained from measured

$$\overline{q^2} = \overline{u^2} + \overline{v^2} + \overline{w^2},$$

measured  $U$  and derived  $\partial\overline{q^2}/\partial x$ ,  $\partial\overline{q^2}/\partial y$  and  $V = -\int(\partial U/\partial x) dy$ . The dissipation was obtained from the isotropic relation  $\epsilon = 15\nu(\partial u/\partial x)^2$  whilst the diffusion was obtained by difference. Although the assumed isotropy of the dissipation term makes it difficult to draw definite conclusions on the shape of the diffusion it is felt that a useful comparison can still be made between similarly obtained energy budgets for different external flow conditions.

*Zero external shear.* The energy budget for  $\lambda = 0$  is compared with that of Klebanoff† (1954) and Charney (1974) for various values of  $T_u$  in figures 12–14 (see figure 27 of Ahmad *et al.* 1975*b*). There is a systematic decrease in the production for  $y/\delta < 0.7$  as  $T_u$  increases. For  $y/\delta > 0.7$ , the trend is reversed. The production becomes zero in the range  $y/\delta = 0.9$ – $1.2$  and there is a decrease in

† See also Bradshaw (1966).

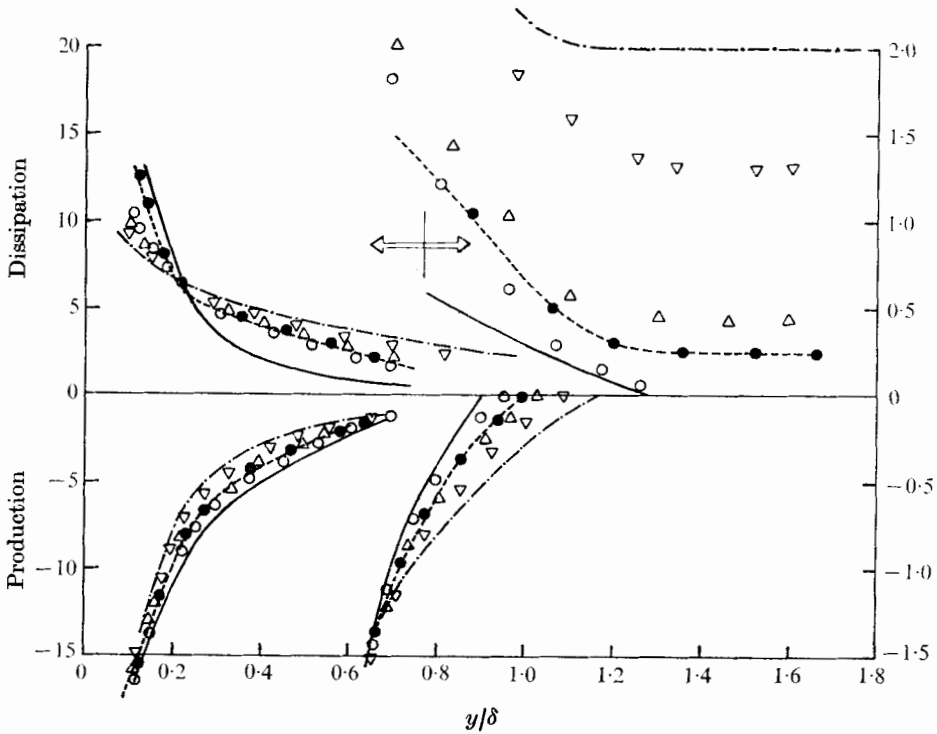


FIGURE 12. Production and dissipation across a boundary layer for zero external shear for different external turbulence levels. Charnay (1974):  $\circ$ , 0.3%;  $\triangle$ , 1.8%;  $\nabla$ , 3.2%;  $-\cdot-\cdot-$ , 4.7%.  $\bullet$ , present results, 1.5%;  $---$ , Klebanoff (1954), 0.2%.

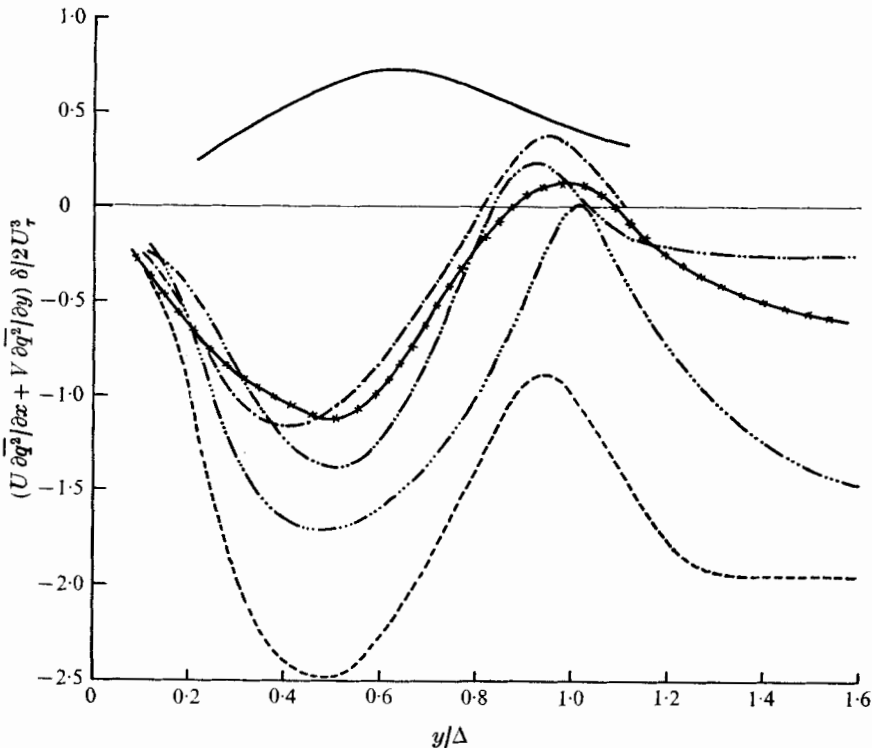


FIGURE 13. Advection across boundary layer for zero external shear for different turbulence levels. Charnay (1974):  $-\cdot-\cdot-$ , 0.3%;  $-\cdot-\cdot-\cdot-$ , 1.8%;  $-\cdot-\cdot-\cdot-\cdot-$ , 3.2%;  $-\cdot-\cdot-\cdot-\cdot-\cdot-$ , 4.7%;  $-*-*-*$ , present results, 1.5%;  $---$ , Klebanoff (1954), 0.2%.

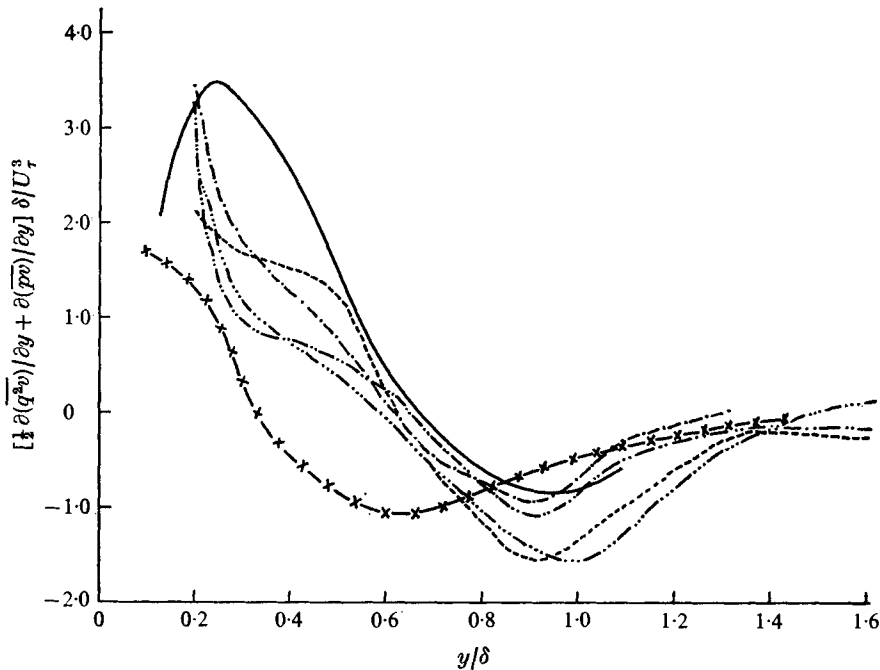


FIGURE 14. Diffusion across boundary layer for zero external shear for different turbulence levels. Symbols same as for figure 13.

the dissipation for  $y/\delta < 0.25$  and a systematic increase for  $y/\delta > 0.25$  as  $T_u$  increases. Outside the boundary layer, the dissipation is approximately constant. Apart from the dissipation values calculated close to the wall, the present results for production and dissipation are in reasonably close agreement with those of Charnay (1974) for  $T_u = 1.8\%$ . In figure 13 it is clear that the gain by advection increases with increasing  $T_u$ . For all turbulence levels, advection tends to increase up to  $y/\delta = 0.5$  and then decreases towards the edge of the boundary layer. In the external flow there is an increase in advection till it becomes constant and, as expected, balances the constant dissipation since both the diffusion and production must be zero in this region. The failure of the diffusion† results in figure 14 to integrate to zero across the layer is partly due to the assumed isotropy of dissipation and partly caused by inaccuracies in the calculation of advection.‡ Figure 14 shows that the turbulent energy diffusion across the boundary layer extends to larger distances from the wall as  $T_u$  increases. At  $y/\delta = 1.0$ , the present advection and diffusion (figures 13 and 14) both indicate a gain in energy which must offset the loss by dissipation as the production is nearly zero. The energy balances for the present data for  $T_u = 1.5\%$  (figure 15) and for Charnay's

† In Charnay's (1974) data, the part of the diffusion due to pressure fluctuations was obtained by difference as the diffusion by  $\overline{q^2 v}$  as measured. However, Charnay's diffusion curves seem to be incorrect as they do not close his energy budget. In figure 26 of Ahmad *et al.* (1975*b*), Charnay's diffusion data have been derived from closure of his budget.

‡ Note for instance the large discrepancy between the advection as obtained by Charnay ( $T_u = 0.3\%$ ) and that of Klebanoff, for a comparable turbulence level.

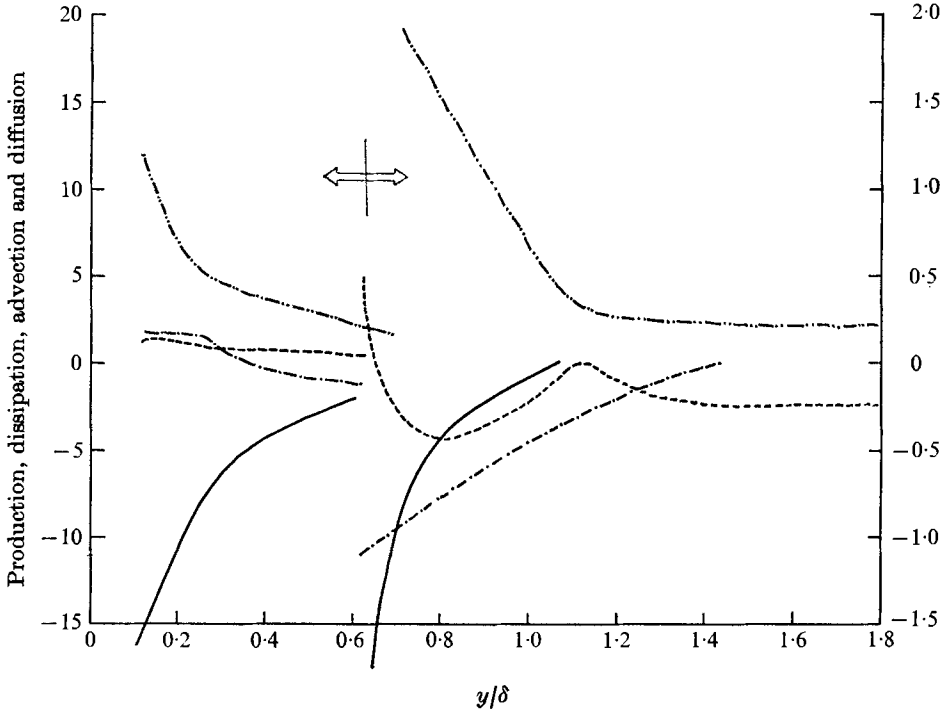


FIGURE 15. Energy balance across boundary layer for zero external shear. —, production; - · - ·, dissipation; - - - -, advection; - - - -, diffusion.

(1974) data for  $T_u = 3.2\%$  show that the details of the balance near the outer edge are quite different from those when  $T_u$  is negligible. In particular, advection has the same sign as diffusion and dissipation is therefore large. This emphasizes that the external turbulence level is a significant parameter in the mechanics of turbulent energy transport.

*Non-zero external shear* ( $\lambda = \pm 6 \text{ s}^{-1}$ ). The energy budgets for  $\lambda = \pm 6 \text{ s}^{-1}$  are shown in figures 16 and 17. There is an increase in the production term for  $y/\delta < 0.4$  compared with the case  $\lambda = 0$ . For  $y/\delta > 0.4$ , a decrease in the production is observed relative to the  $\lambda = 0$  case. There is also a corresponding increase in the inner region and a decrease in the outer region of the dissipation. The production becomes zero in the constant-velocity region and then increases outside the boundary layer before assuming a constant value. This constant production for  $\lambda = -6 \text{ s}^{-1}$  is about one-fifth of that for  $\lambda = +6 \text{ s}^{-1}$  as  $|(\overline{uv})_1|$  and  $\delta/U_7^3$  both are smaller for  $\lambda < 0$ . In the case  $\lambda > 0$  (figure 20) the dissipation first decreases, then increases and ultimately becomes constant, while for negative shear (figure 17), the dissipation gradually decreases and attains a constant value without becoming zero. Diffusion becomes zero at  $y/\delta = 1.25, 1.32$  and  $1.42$  for  $\lambda = -6 \text{ s}^{-1}, 6 \text{ s}^{-1}$  and  $0$  respectively (figures 17, 16 and 15), indicating that the extent of diffusion of turbulent energy is slightly reduced by the presence of an external shear. Up to  $y/\delta = 0.6$ , the diffusion is not strongly affected by the shear but there is a decrease in the gain by diffusion for  $y/\delta > 0.6$  when

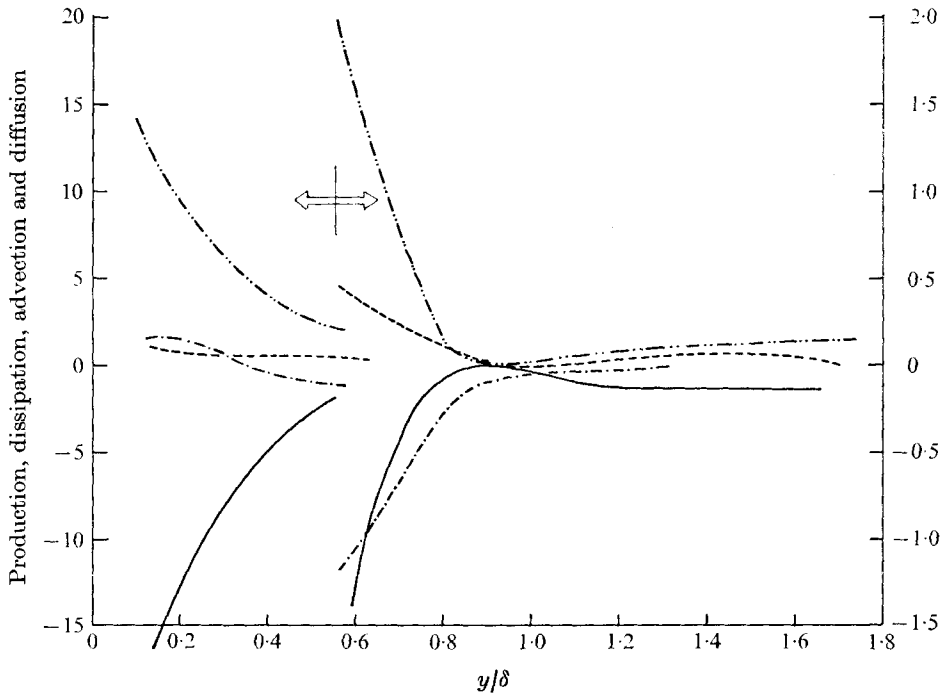


FIGURE 16. Energy balance across boundary layer for positive external shear. Symbols same as for figure 15.

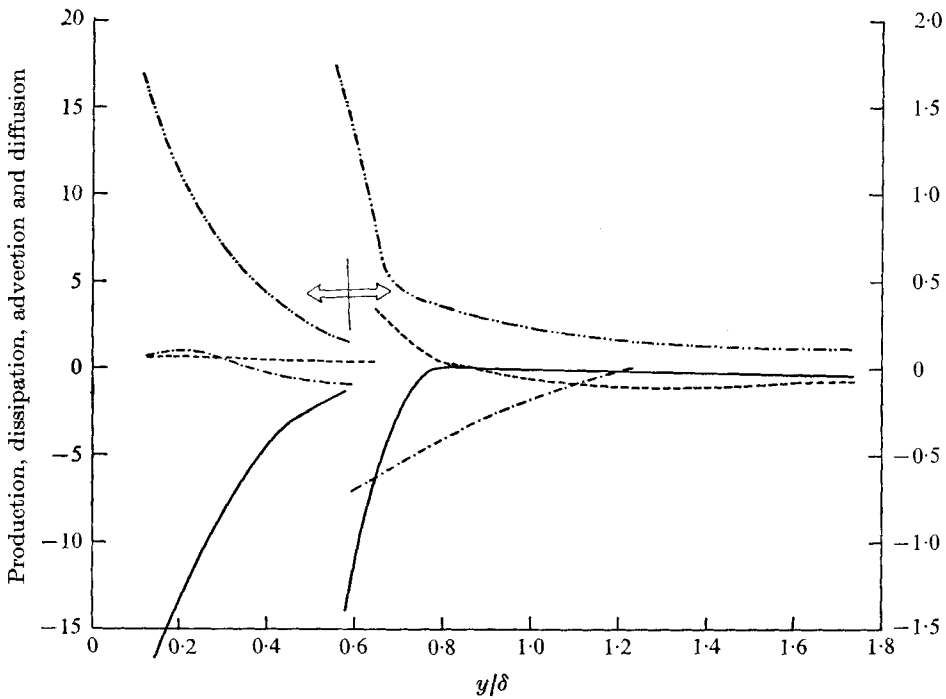


FIGURE 17. Energy balance across boundary layer for negative external shear. Symbols same as for figure 15.

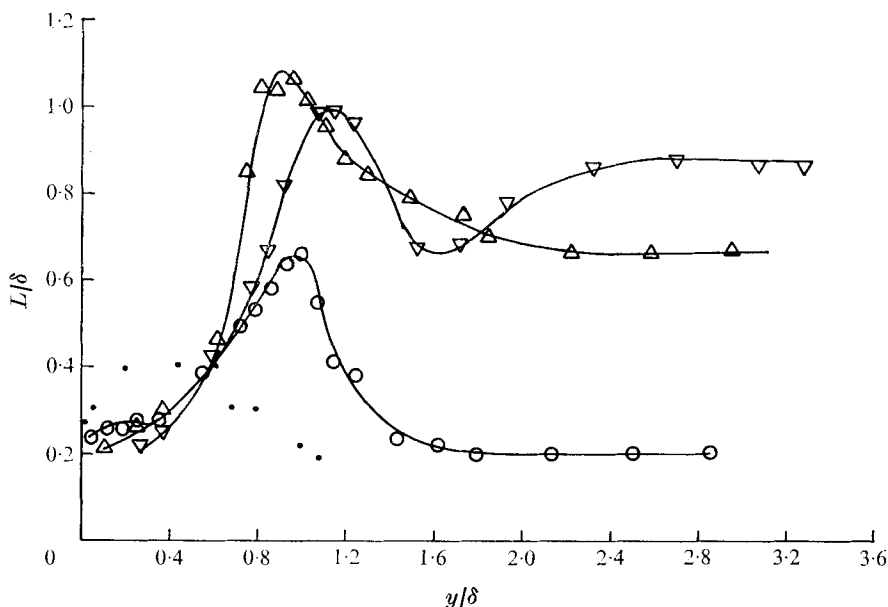


FIGURE 18. Longitudinal integral length scale across boundary layer.

●,  $\lambda = 0$ , Antonia (1969). Present results: ○,  $\lambda = 0$ ; △,  $\lambda = +6 \text{ s}^{-1}$ ; ▽,  $\lambda = -6 \text{ s}^{-1}$ .

the external shear is applied and this decrease is more pronounced for  $\lambda = +6 \text{ s}^{-1}$  than for  $\lambda = -6 \text{ s}^{-1}$ . The advection is also not strongly affected for  $y/\delta < 0.6$ . There is a gain by advection in the region  $y/\delta > 0.6$  in zero shear (figure 15) and a slight loss and gain with positive and negative shear (figures 16 and 17) respectively for  $y/\delta > 0.85$ . A detailed energy budget for large values of  $y/\delta$  (given in Ahmad *et al.* 1975*b*) provides good support for the homogeneity of the external shear-flow turbulence in that the diffusion term, obtained by difference, is zero.

#### 6.4. Turbulence length scales

The integral length scales presented in this subsection are obtained from the one-dimensional spectral density of  $u$ , viz.  $L = \pi\phi_u(\omega = 0)/2\overline{u^2}$ . All the measured spectra exhibit a plateau in  $\phi_u$  at the lowest observed frequencies (down to 1 Hz), so that  $L$  seems to be unambiguously defined in all cases. The length scales for  $\lambda = \pm 6 \text{ s}^{-1}$  are in good agreement outside the boundary layer and are approximately three times the value for  $\lambda = 0$ . This difference is probably a result of different experimental initial conditions. Distributions of  $L/\delta$  vs.  $y/\delta$  are shown in figure 18. The values of  $L/\delta$  obtained by Antonia (1969) for  $T_u \simeq 0.05\%$ , by Johnson (1959) for  $T_u \simeq 0.07\%$  and by Fulachier (1972) for  $T_u \simeq 0.12\%$  are considerably higher than the present values for  $y/\delta < 0.5$ , which indicates that the external length scale exerts an appreciable influence on  $L$ . It is difficult to assess with confidence any possible further effect due to the external shear in view of the uncertainty in the choice of  $\delta$ , and the different length scales in the present three external conditions. However it is possible that the combination of a larger external length scale and a Reynolds shear stress

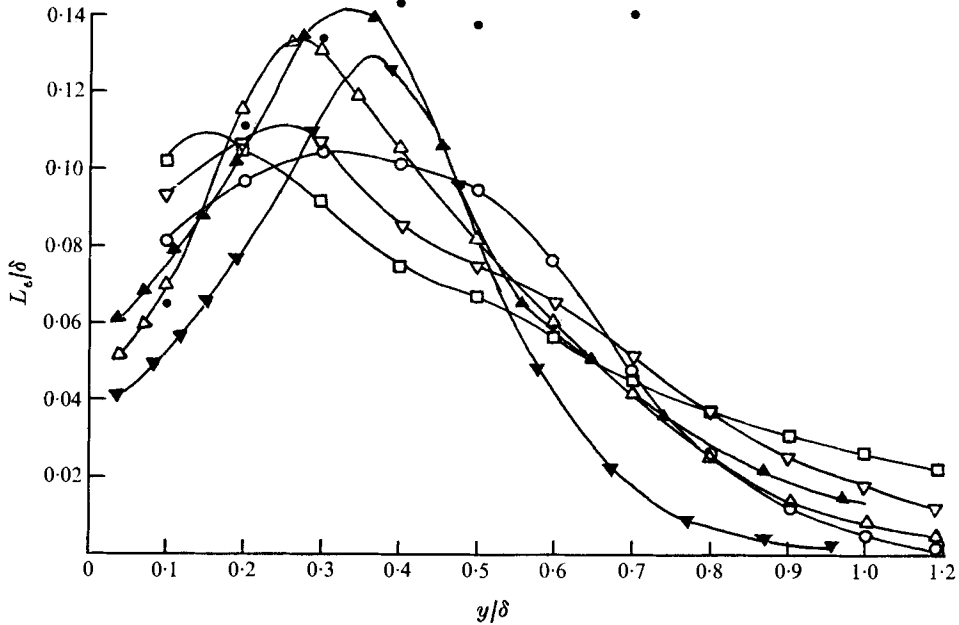


FIGURE 19. Dissipation length scale across boundary layer for different external turbulence levels. Charnay *et al.* (1972) ( $\lambda = 0$ ):  $\circ$ , 0.3%;  $\nabla$ , 3.2%;  $\square$ , 4.7%.  $\bullet$ , Klebanoff (1954), 0.2% ( $\lambda = 0$ ). Present results:  $\triangle$ , 1.5% ( $\lambda = 0$ );  $\blacktriangle$ , 1.3% ( $\lambda = +6 \text{ s}^{-1}$ );  $\blacktriangledown$ , 1.6% ( $\lambda = -6 \text{ s}^{-1}$ ).

in the outer flow of opposite sign to that in the boundary layer may lead to a reduction in the correlation of  $u$  (and possibly other components) in the boundary layer.

Another length scale that may be thought to characterize the energy-containing eddies is the dissipation length scale  $L_\epsilon$ , defined as  $L_\epsilon = |-\overline{uv}|^{1/2}/\epsilon$ . Present distributions of  $L_\epsilon$  are compared with those of Klebanoff (1954) and Charnay *et al.* (1973). In figure 19. The straight line given by  $L_\epsilon/\delta = 0.4y/\delta$  lies well below the data, which suggests that the mixing-length concept becomes less tenable as the external turbulence level increases. The breakdown of this concept is consistent with the previously noted increase in dissipation and reduced production as  $T_u$  increases. Outside the layer,  $L_\epsilon/\delta$  becomes zero at  $1.4\delta$  for  $\lambda = 0$ , while for  $\lambda = \pm 6 \text{ s}^{-1}$  it increases before becoming constant, the value for  $\lambda = +6 \text{ s}^{-1}$  being about 5.5 times that for  $\lambda = -6 \text{ s}^{-1}$ . The large discrepancy between  $L_\epsilon$  and  $L$  seems to be due to the higher stresses and lower dissipation values for  $\lambda = +6 \text{ s}^{-1}$  than for  $\lambda = -6 \text{ s}^{-1}$ . For all three values of  $\lambda$  considered here, the length scale  $(\overline{q^2})^{1/2}/\epsilon$  is nearly  $4.5L$  in the external flow, which is in agreement with grid turbulence data and the results of Charnay (1974). However, the present values of  $L$  in the boundary layer are higher than those inferred from Charnay's data for the  $u$ -component transverse integral length scale (assumed equal to  $\frac{1}{2}L$ ) for the same  $T_u$ . In the present external flow ( $\lambda = 0$ ), the value of  $L/\delta$  is about 0.5, which is twice that in Charnay's flow. Charnay's data clearly indicate that, in the inner layer, the increase in  $L/\delta$  is larger with an increase in

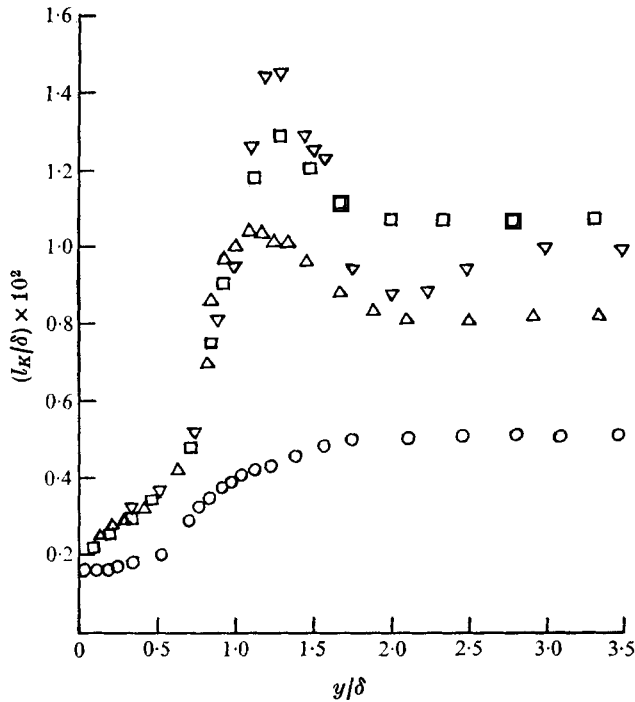


FIGURE 20. Lateral distribution of Kolmogorov length scale.  $\circ$ ,  $x = 1.63$  m,  $\lambda = -6$  s $^{-1}$ ;  $\triangle$ ,  $x = 1.63$  m,  $\lambda = 0$ ;  $\nabla$ ,  $x = 1.63$  m,  $\lambda = +6$  s $^{-1}$ ;  $\square$ ,  $x = 2.21$  m,  $\lambda = +6$  s $^{-1}$ .

the external length scale for the same  $T_u$  than with an increase in  $T_u$  for the same external scale. Figure 19 shows that  $L_e/\delta$  is not significantly affected by  $T_u$  (as suggested by Huffman *et al.* 1972) or  $\lambda$ . Hence, as noted by Bradshaw (1974), the effects of free-stream turbulence are expected to depend more critically on the magnitude of the length scale than on  $T_u$ .

The Kolmogorov length scale  $l_K = (\nu^3/\epsilon)^{1/4}$ , normalized with  $\delta$ , is plotted against  $y/\delta$  in figure 20. Outside the layer,  $l_K$  is greater for  $\lambda = \pm 6$  s $^{-1}$  than for  $\lambda = 0$ , which is consistent with the smaller values of dissipation when  $\lambda = \pm 6$  s $^{-1}$ . The main feature of figure 20 is that the distributions of  $l_K$  for  $\lambda = \pm 6$  s $^{-1}$  have the same qualitative trend as those for  $L$  or  $L_e$ . For  $\lambda = 0$  however, the peak in  $L$  or  $L_e$  is no longer apparent in the  $l_K$  distribution. Hence, as a result of the dissipation being nearly zero in the interaction region,  $l_K$  seems to mirror the behaviour of  $L$  better than that of  $L_e$ .

## 7. Summary of results and concluding comments

Measurements in the external uniform turbulent shear flow with  $\lambda = +6$  s $^{-1}$  are found to be in agreement with the more detailed investigation of Mulhearn (1971). In particular, the turbulence length scales are found to increase linearly with  $x$  and all the Reynolds stresses become approximately constant at

$$x\lambda/U_c \simeq 2.4$$

and begin to increase when  $x\lambda/U_c > 4$ . The rate of increase with  $x$  of the longitudinal normal stress is significantly higher than that for the other stresses, which seems to point to the ineffective role of the pressure fluctuations in redistributing the turbulent energy among the various components. Measurements in the boundary layer are made over the relatively small streamwise region where the external turbulence field was quasi-homogeneous.

For the case of no external shear, the measurements are essentially in agreement with those available in the literature. The skin friction  $c_f$  is increased when compared with that in a layer with  $T_u \simeq 0$  at the same value of  $R_\Theta$ . Distributions of mean velocity, Reynolds stress and energy balance in the inner part of the layer are essentially identical with those for  $T_u = 0$ . However the turbulence length scale in the inner layer is found to be lower than that measured for  $T_u = 0$ . This result is different from that of Charnay *et al.* (1972), who find an increase in the transverse length scale when either  $T_u$  or the external length scale is increased. The present distribution of  $L/\delta$  also overshoots significantly its free-stream value near  $y = \delta$ .

With an external positive or negative shear, the distributions of mean velocity, Reynolds stresses and the energy budget in the inner layer are the same as for  $\lambda = 0$ . Except near the edge of the layer, the shape of the velocity defect distribution is similar to that for  $\lambda = 0$  at the same value of  $T_u$ . The almost negligible effect of  $\lambda$  relative to that of  $T_u$  on the 'wake' component of the mean velocity profile is more pronounced in the data of Masuda *et al.* (1972), who used larger values of  $\lambda$  ( $= \pm 60 \text{ s}^{-1}$ ). At the edge of the layer, there is a small region where the velocity gradient is zero, for both negative and positive  $\lambda$ . This rather unexpected (at least for  $\lambda > 0$ ) result is supported by the shear-stress distribution, which is approximately zero in this region before increasing to its constant external-flow value.

Distributions of the differences between the local Reynolds stresses and the corresponding values in the external shear flow tend to show, when plotted *vs.*  $y/\Delta$ , reasonable similarity for the small range of  $x$  investigated here. This similarity is better when  $\lambda > 0$ , when the advection term in the outer stream is negligible, than when  $\lambda < 0$ , when the advection is almost equal to the dissipation in the external flow. For  $\lambda > 0$ , the distributions of Reynolds stresses in the outer part of the layer are larger than in the case  $\lambda = 0$ , whilst for  $\lambda < 0$  they are significantly smaller. There does not appear to be an effect of  $\lambda$ , additional to that of  $T_u$ , on the integral length scale in the inner part of the layer.

In his survey paper, Bradshaw (1974) concluded that 'the detailed mechanism of free-stream turbulence effects is not understood, even qualitatively'. The addition of a shear to the external-flow turbulence is not likely to make our understanding better. Although the present measurements tend to indicate that the extra complications introduced by the external shear are probably small, *there is a definite need for further experiments, particularly with higher values of  $\lambda$ .* Also, a systematic study of the influence of the external-flow length scale on the turbulence structure of the boundary layer would be of particular interest. A detailed study of the interaction region between the boundary layer and the external shear flow would best be carried out with the use of a conditional

sampling technique (e.g. Charnay 1974) and the introduction of a passive scalar contaminant in one of the flows. Fabris (1974) has used this method to study the interaction between two wakes, while Dean (1974) has applied it to investigate the interaction of shear layers in a duct flow. Comparison between these various interactions would certainly be useful.

This work was supported by the Australian Research Grants Committee and the Australian Institute of Nuclear Science and Engineering.

## REFERENCES

- AHMAD, Q. A., LUXTON, R. E. & ANTONIA, R. A. 1975*a* *J. Appl. Mech. Trans. A.S.M.E.*, **97**, 283.
- AHMAD, Q. A., LUXTON, R. E. & ANTONIA, R. A. 1975*b* *Chas Kolling Res. Lab., Dept. Mech. Engng, Univ. Sydney, Rep. no. TNF-75*.
- ANTONIA, R. A. 1969 Ph.D. thesis, Department of Mechanical Engineering, University of Sydney.
- BRADSHAW, P. 1966 *Nat. Phys. Lab. Aero. Rep. no. 1184*.
- BRADSHAW, P. 1974 *Imperial College Aero. Rep. no. 74-10*.
- CHAMPAGNE, F. H., HARRIS, V. G. & CORRSIN, S. 1970 *J. Fluid Mech.* **41**, 81.
- CHARNAY, G. 1974 Thèse Docteur des Sciences, Université de Lyon.
- CHARNAY, G., COMTE-BELLOT, G. & MATHIEU, J. 1972 *AGARD Conf. Proc. no. 93*.
- CHARNAY, G., COMTE-BELLOT, G. & MATHIEU, J. 1973 *C. R. Acad. Sci. Paris, A* **277**, 1119.
- CLAUSER, F. H. 1954 *J. Aero. Sci.* **21**, 91.
- CLAUSER, F. H. 1956 *Adv. Appl. Mech.* **4**, 1.
- COLES, D. 1962 *RAND Corp. Rep. no. R-403-PR*.
- COSTIN, G. D. L. 1971 *Proc. 4th Austr. Conf. Hydraul. Fluid Mech.* Paper 61.
- DEAN, R. B. 1974 *Proc. 5th Austr. Conf. Hydraul. Fluid Mech., Christchurch, New Zealand*, vol. 1, p. 340.
- FABRIS, G. 1974 Ph.D. thesis, Department of Mechanical Engineering, Illinois Institute of Technology.
- FULACHIER, L. 1972 Thèse Docteur des Sciences, Université de Provence.
- GORLIN, S. M. & ZRAZHEVSKII, I. M. 1972 *Mech. Zh. Moscow, Gaza*, **4**, 52.
- GREEN, J. E. 1972 *R.A.E., Tech. Rep. no. 72201*.
- HEAD, M. R. & RAM, V. V. 1971 *Aero. Quart.* **22**, 295.
- HWANG, W. S. 1971 Ph.D. thesis, School of Engineering and Applied Science, University of Virginia.
- HUFFMAN, G. D., ZIMMERMAN, D. R. & BENNETT, W. A. 1972 *AGARD Conf. Proc. no. 164*.
- JOHNSON, D. S. 1959 *J. Appl. Mech., Trans. A.S.M.E.* **26**, 325.
- KLEBANOFF, P. S. 1954 *N.A.C.A. Tech. Note*, no. 3178.
- KLINE, S. J., LISIN, A. V. & WAITMAN, B. E. 1960 *N.A.S.A. Rep. no. D-368*.
- MASUDA, S., SASAKI, N., ARIGA, I. & WATANABE, I. 1972 *2nd Int. J.S.M.E. Symp. Fluid Machinery & Fluidics, Tokyo*.
- MULHEARN, P. J. 1971 Ph.D. thesis, Department of Mechanical Engineering, University of Sydney.
- MULHEARN, P. J. & LUXTON, R. E. 1970 *Chas Kolling Res. Lab., Dept. Mech. Engng, Univ. Sydney, Rep. no. TNF-19*.
- MULHEARN, P. J. & LUXTON, R. E. 1975 *J. Fluid Mech.* **68**, 577.
- RICHARDS, H. K. 1971 Ph.D. thesis, School of Engineering and Applied Science, University of Virginia.

ROSE, W. G. 1966 *J. Fluid Mech.* **25**, 97.

ROSE, W. G. 1970 *J. Fluid Mech.* **44**, 767.

TOWNSEND, A. A. 1956 *The Structure of Turbulent Shear Flow*. Cambridge University Press.

TOWNSEND, A. A. 1965 *J. Fluid Mech.* **22**, 773.

TOWNSEND, A. A. 1966 *J. Fluid Mech.* **26**, 255.

WOOD, D. 1975 M.S. thesis, Department of Mechanical Engineering, University of Sydney.